COMPUTING THE TORTUOSITY OF CANCELLOUS BONE CAVITY NETWORK THROUGH FLUID VELOCITY FIELD

Waldir L. Roque* and Fabiano G. Wolf **

*Departamento de Computação Científica, UFPB, João Pessoa, Brazil
**Centro de Engenharias da Mobilidade, UFSC, Joinville, Brazil

e-mails:roque@ci.ufpb.br; fabiano.wolf@ufsc.br

Abstract: Tortuosity is a very important parameter for the characterization of fluid flow in porous media. Cancellous bone is a spongy structure that can be modelled as a two phase porous medium, where the solid phase corresponds to the trabecular bone and the fluid phase comprises the marrow. The microcirculation of blood in cancellous bone plays an important role in bone physiological responses. In this paper we estimate the tortuosity of the marrow cavity network for a set of μCT distal radius samples using the fluid velocity field (FVF) and compare the FVF results with the tortuosities obtained by the geodesic reconstruction (GR) algorithm. It has been shown that there is a strong correlation (r = 0.9396) between FVF and GR and the Bland-Altman plot indicates a good agreement of these techniques.
Keywords: Tortuosity, cancellous bone, velocity field, geodesic reconstruction, osteoporosis.

Introduction

With the growing of the elderly population a noticeable increase of osteoporosis has been observed by the medical community. The problems caused by osteoporosis is the bone mass loss and degradation of the trabecular structure. One severe consequence of osteoporosis is bone fracture due to bone fragility. It is estimated that osteoporosis affects over 75 million people in USA, Europe and Japan, together, with a very high cost to the health care systems. Total cost of fragility fractures in France, Germany, Italy, Spain, Sweden and UK together is around 31 billion of euros per year and just in the US more than 2.05 million fragility fractures occur per year with a cost over 16.9 billion of dollar.

The bone, seen as an organ, is in fact classified as cortical and cancellous. The cortical bone is an external compact shell and the internal sponge-like one forms the cancellous part. Cancellous bone is actually seen as composed of trabecular bone and its marrow counterpart. The trabecular bone form a network with a more active remodelling process than the cortical and can be seen as the solid part (grain) of a two phase porous medium, while the marrow is essentially fat and represents the fluid part (pore) of the cancellous bone.

Several morphological, geometrical and mechanical parameters can be extracted from the trabecular structure in an attempt to provide information about its characterization and mechanical behavior. The trabeculae form a rather tortuous network structure. On the other hand, cancellous bone is a very complex tissue and to understand its dynamics one need to investigate and examine not just its mechanical aspects, but its physiological too. The microcirculation of blood through bone is important to deliver nutrients and oxygen, which are essential to trabecular remodeling by stimulating osteoclastic activity, increasing mineral deposition, maintenance of bone health and repair of fracture and injuries [1]. The regulation of blood flow is an important process to control the rate of nutrient intake and release, as well as release of tissue waste. Fluid flow in the interstitial fluid in bone seems to produce streaming potential, which acts stimulating osteoblasts to create new bone. It has been observed with methods that the intraosseous blood flow ranges from 5 to 20 ml/min/100g of bone, in humans and animals. Nevertheless, the blood flow circulation in bone is not yet very well understood in humans and just a little is known about the tortuosity of the marrow cavity network.

In fact, in [2] the tortuosity of marrow cavities were obtained using audiofrequency pulses applied to five bone replicas constructed by stereolithography 3D printing. The replicas were from different bone sites and none was from distal radius, as will be the samples in the present study.

In this paper we estimate the marrow cavity tortuosity of 15 distal radius cancellous bone samples using the fluid velocity field (FVF) technique [3]. The results are compared to those ones previously obtained by the application of the geodesic reconstruction (GR) algorithm [4].

Materials and methods

In this section we introduce the notion of tortuosity, briefly discuss the FVF technique and specify the cancellous bone samples used in this study.

Tortuosity – In [5] several definitions of tortuosity

are presented and discussed according to the field of interest. However, the simplest definition is the ratio of the geodesic length of a path between two connected points $\{a, b\}$, $L_G(a,b)$, to the Euclidian length $L_E(a,b)$,

$$\tau(a,b) = \frac{L_G(a,b)}{L_E(a,b)} \quad (1)$$

For the computation of the tortuosity by geodesic reconstruction algorithm, the L_E will be considered as the distance between two parallel reference planes. This allows to classify an object that is not orthogonal to the reference planes as having a tortuosity such that $\tau(a,b) \geq 1$.

Fluid velocity field – The FVF technique as a mean to estimate the hydraulic tortuosity was recently discussed in [6, 9] for a general porous medium. The FVF hydraulic tortuosity is computed as

$$\tau = \frac{\langle v \rangle}{\langle v_z \rangle} \quad (2)$$

where $\langle v \rangle = \int_V v(\boldsymbol{r}) d^3\boldsymbol{r}$ is the fluid average magnitude of the intrinsic velocity over the pore space volume V and $\langle v_z \rangle$ is the average of the velocity component along the macroscopic flow direction. To implement this technique to estimate the tortuosity of a pore network, equation (2) is discretized, the Lattice-Boltzmann method (LBM) [10, 11] is used to run numerical simulations up to reach steady state, when the tortuosity is estimated.

Algorithm implementations – The algorithm to compute the tortuosity using the geodesic reconstruction can be found in [4, 12].

The algorithm to compute the tortuosity using the FVF has been implemented in the framework of the Lattice-Boltzmann method with Bhatnagar-Gross-Krook (BGK) operator, for which the governing kinetic equation is given by

$$f_i(\boldsymbol{x} + \boldsymbol{c}_i\delta t, t + \delta t) - f_i(\boldsymbol{x}, t) = \frac{\delta t[f_i(\boldsymbol{x}, t) - f_i^{eq}(n, \boldsymbol{u})]}{\gamma}, \quad (3)$$

where f_i is the particle distribution function that gives the number of particles at site $\boldsymbol{x}$ and time t with velocity c_i (i = 0,...,18) in a discrete set of velocities. The function f_i^{eq} is the particle local equilibrium distribution defined in terms of the particle number density, n, and local macroscopic velocity, $\boldsymbol{u}$, and given in reference [11]. Lattice units are used to represent the model parameters, in which the lattice spacing (ls), δx, and time step (ts), δt, are distance between two adjacent sites and time between two consecutive collisions, respectively. Here, δx = 1 ls and δt = 1 ts. The constant γ is the relaxation time which is related to the kinematic viscosity [11], and it is adjusted in this work to $\gamma = (2+\sqrt{3})/4 \approx 0.933$ ts.

To force and maintain the fluid flow through the medular cavities in a body, a force is added locally at each timestep by using the following expression for the equilibrium velocity, $\boldsymbol{u}^{eq}$:

$$\boldsymbol{u}^{eq}(\boldsymbol{x}) = \boldsymbol{u}(\boldsymbol{x}) + \frac{\gamma \boldsymbol{F}_g}{n}, \quad (4)$$

where $\boldsymbol{F}_g = n(\boldsymbol{x})\boldsymbol{g}$. The components g_x, g_y and g_z are set according to the intended macroscopic flow direction. For instance, for a fluid flow in x-direction, $g_x = g$, and $g_y = g_z = 0$. In all simulations the scalar g is equal to 1×10^{-6}ls/ts^2, keeping the local fluid velocities with low values.

The boundary conditions used are based on keeping a constant number density, n_I, at the inlet and outlet boundaries by imposing a local equilibrium distribution function $f_i^{eq}(n_I, \boldsymbol{u}_I)$, where the value of the imposed velocity, $\boldsymbol{u}_I$, is obtained by assessing the nearest site from the boundary inward domain. Supposing the fluid flow is parallel to the axis x, the equilibrium distribution functions imposed at the inlet, f_i^I, and outlet, f_i^O, sites, respectively, will be given by

$$\begin{aligned} f_i^I(n_I, \boldsymbol{u}_I) &= f_i^{eq}\big(n_I, \boldsymbol{u}(\boldsymbol{x} + \Delta\boldsymbol{x}, \boldsymbol{y}, \boldsymbol{z})\big) \\ f_i^O(n_I, \boldsymbol{u}_I) &= f_i^{eq}\big(n_I, \boldsymbol{u}(\boldsymbol{x} - \Delta\boldsymbol{x}, \boldsymbol{y}, \boldsymbol{z})\big). \end{aligned} \quad (5)$$

It is assumed periodic boundary conditions for all other boundaries of the domain. The simulations were done considering getting steady-state conditions after the following convergence criterion to be reached

$$\frac{\sqrt{\sum_{\boldsymbol{x}}[\boldsymbol{u}(\boldsymbol{x},t) - \boldsymbol{u}(\boldsymbol{x},-500)]^2}}{\sqrt{\sum_{\boldsymbol{x}}[\boldsymbol{u}(\boldsymbol{x},t)]^2}} < \varepsilon. \quad (6)$$

After some preliminary results, it was observed that $\varepsilon = 1 \times 10^{-5}$ would be a good choice, since it allows getting good results with acceptable computational times. The consumed time for each sample varied from around 3 to 14 hours using a custom made computer program written in C++ with OpenMP technology, running in a quad-core PC.

Cancellous bone samples

The GR and FVF algorithms were applied to estimate the tortuosity of marrow cavities of a set of 15 distal radius μCT *ex-vivo* samples. The technical details about the samples preparation are described in [13].

The cancellous bone image samples were binarized and then considered as a two phase porous medium, where the marrow cavities are the pores, here interpreted as the white voxels, and the trabecular bone network are the white voxel complements. Figure 1 shows the 3D reconstruction of the trabecular bone network of two samples. The volume complement of the trabecular bone corresponds to the marrow cavities. It can be easily seen that sample 265 (left) has smaller marrow cavities than sample 269 (right), i.e., the trabecular structure of sample 269 is more deteriorated.

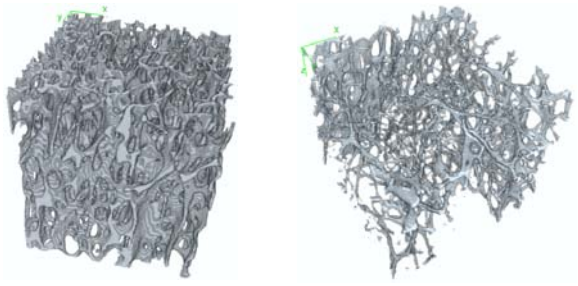

Figure 1: 3D reconstructions of distal radius trabecular network of 265 (L) and 269 (R) samples.

Results

The tortuosities of the marrow cavities for the 15 samples were obtained by the application of the GR and FVF algorithms in the (+z)-direction, corresponding to the distal-proximal direction, which was chosen as the fluid direction for simulations. The tortuosity values and the marrow cavities volume fraction (MVF) are given in Table 1. The MVF is defined as

$$MVF = \frac{Marrow\ cavity\ volume}{Total\ volume}, \qquad (7)$$

where the marrow cavity volume is estimated by the number of voxels that form the cavities and the total volume is the sample volume. Notice that the MFV is in fact the porosity of the sample.

From Table 1 the minimum FVF and GR tortuosities occur for the 269 sample, which is actually the sample that presents the worst trabecular structure, or else, the largest marrow cavities. On the other hand, sample 265 shows a very compact trabecular network, what is reflected in a lower MFV and higher marrow cavity FVF and GR tortuosities.

Table 1: MVF and tortuosities of the samples estimated by FVF and GR algorithms.

Sample	MVF	$\tau_{+z\,(FVF)}$	$\tau_{+z\,(GR)}$
254	0.921	1.04538	1.02018
255	0.926	1.04491	1.01979
256	0.913	1.04592	1.02111
262	0.900	1.04576	1.02229
263	0.918	1.05608	1.02375
264	0.893	1.07036	1.02968
265	0.857	1.05289	1.03024
266	0.896	1.05517	1.02533
267	0.878	1.06085	1.02912
268	0.935	1.04937	1.02048
269	0.962	1.02360	1.00985
270	0.937	1.03810	1.01674
271	0.925	1.03952	1.01793
272	0.928	1.04797	1.02040
273	0.965	1.02693	1.00971

Discussion

To be able to compare the tortuosities obtained by the FVF algorithm, we have also estimated the marrow cavity tortuosities of each sample using the geodesic reconstruction algorithm [4]. The results given in Table 1 show that for cancellous bone with larger marrow cavities, corresponding to a higher porosity, the pore network becomes more straight getting the tortuosity closer to $\tau \approx 1$. On the other hand, higher marrow cavity tortuosity is an indication of a better structured network.

The Pearson correlation between FVF and GR tortuosities is quite good, $r = 0.9396$, $p < 0.0001$, and 95% confidence interval ranging from 0.8239 to 0.9801. To be able to compare the limits of agreement (LoA) between the two techniques, the Bland-Altman graph is presented in Figure 2. From the graph it can be seen that tortuosities obtained by both techniques are reasonably comparable, as nearly 95% of the difference points are inside the lower and upper lines defining the LoA. However, as the line of equality (red dashed line at zero) lies outside 95% confidence interval, this is an indication that there might be a significant systematic difference between the two techniques.

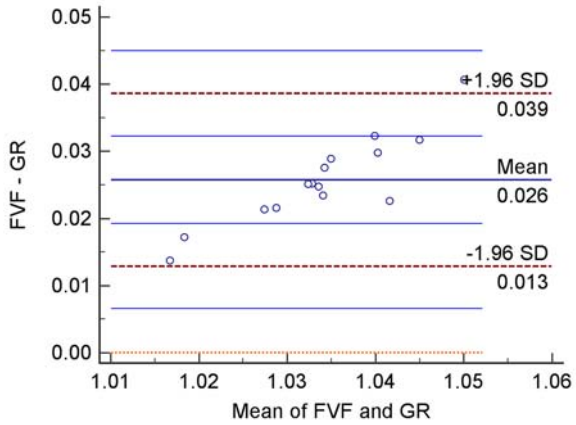

Figure 2: Bland-Altman plot for FVF and GR tortuosities.

In terms of perfusion in marrow cavities, the tortuosity affects the transport of mass and for larger marrow cavities the fluid flow streamlines are straighter as compared to smaller cavities. Figure 4 illustrates the fluid flow streamline velocities in 265 and 269 samples, where the blue streamlines represent low, green medium and red high velocities. The red streamlines have Vmax[265] = 0.000816 lu/ts, and Vmax[269] = 0.005486 lu/ts, where lu means lattice units, corresponding to the distance between the lattice nodes, and ts means time step, corresponding to the model time unit defined as the time for a particle to travel from one node to the other. The z length sizes of 265 and 269 samples are 300 lu and 239 lu, respectively.

In Figure 3, it can be seen some red streamlines in sample 269. This sample has cavities that are much

larger than those in sample 265. As the cavities are larger and longer in the *z*-direction, the tortuosity of the cavities are smaller, what provide less resistivity to the fluid flow.

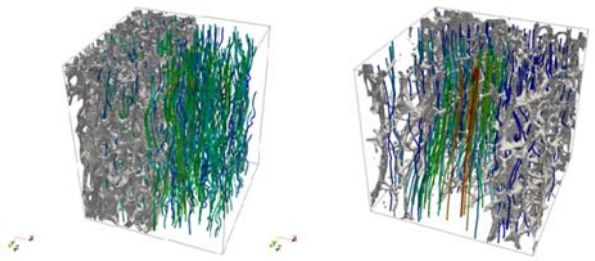

Figure 3: Velocity streamlines of 265 (L) and 269 (R) samples.

Conclusion

The tortuosity is a parameter that plays an important role for the fluid flow along cancellous bone marrow cavities. In this paper, an important contribution is the fact that an alternative technique, the fluid velocity field (FVF), can be applied to estimate the tortuosity of the marrow cavity network, and an algorithm has been implemented in a custom made computational program in C++ to this purpose.

The tortuosity results obtained with the FVF algorithm were compared to those ones previously obtained by the geodesic reconstruction algorithm. It has been shown that these techniques have a high correlation, and according to the Bland-Altman graphs these techniques compare reasonably well, despite of a significant systematic difference. As neither techniques can be currently considered as more accurate than the other as none of them are considered the reference technique, it is not possible to discard any one of them as a potential technique to estimate marrow cavity tortuosity.

Further work needs to be done to see which technique performs better and how the tortuosity actually influences the microcirculation of blood in cancellous bone.

Acknowledgements

W. R. Roque thanks Dr. S. Felipussi for some discussions on Bland-Altman plotting.

References

[1] Laroche M, Intraosseous circulation from physiology to disease, Joint Bone Spine, 2002; 69 pp. 262-269.

[2] Attenborough K, Shin HC, Qin Q and Fagan MJ, Measurements of tortuosity in stereolithographical bone replicas using audiofrequency pulses (L), J. Acoust. Soc. Am., 2005; 118 pp. 2779-2782.

[3] Duda A, Koza Z and Matyka M, Hydraulic tortuosity in arbitrary porous media flow, Physical Review E, 2011; 84, 036319.

[4] Roque WL, Arcaro K and Alberich-Bayarri A, Mechanical competence of bone: a new parameter tograde trabecular bone fragility from tortuosity and elasticity. IEEE Transactions on Biomedical Engineering. 2013; 60 ,pp. 1363–1370.

[5] Clennell MB, Tortuosity: a Guide Through the Maze. In: Developments in Petrophysics, vol. 122, Geological Society, London; 1997, pp. 299-344.

[9] Matyka M and Koza Z, How to Calculate Tortuosity Easily?, In: Porous Media and Its Applications in Science, Engineering, and Industry. AIP Conf. Proc. 1453, 2012, pp. 17-22.

[10] Qian YH, d'HumiFres D, Lallemand P, Lattice BGK Models for Navier-Stokes Equation. Europhys. Lett. 17 (6) (1992) 479–484.

[11] Chen H, Chen S, Matthaeus WH, Recovery of the Navier-Stokes equations using a lattice-gas Boltzmann method. Phys. Rev. A 45 (8) (1992) R5339–R5342.

[12] Roque, WL, Arcaro K e Freytag, I.,Tortuosidade da rede do osso trabecular a parir da reconstrução geodésica de imagens binárias tridimensionais. Anais do XI Workshop de Informática Médica, 2011, pp. 1708-1717.

[13] Laib A, Beuf O, Issever A, Newitt DC and Majumdar S, Directmeasures of trabecular bone architecture from MR images, Adv. Exper. Med. Biol., 2001;496, pp. 37–46.